Thermal Resistance of Electrical Insulation for Bolted and Clamped Discrete Power Devices

Mikel Garcia-Poulin, Mehran Ahmadi,
Majid Bahrami*
Laboratory for Alternative Energy Conversion,
School of Mechatronic Systems Engineering
Simon Fraser University
250-13450 102 Avenue Surrey, BC, Canada
* mbahrami@sfu.ca

Eric Lau, Chris Botting
Delta-Q Technologies Corp.
3755 Willingdon Ave. Burnaby, BC, Canada

Abstract

In power electronic systems, TO-220 packaged electronic devices are bolted or clamped to a metal heat sink for cooling. When mounting high voltage TO-220 devices to touch-safe heat sinks, electrical insulation must be used between the device and the heat sink. This paper experimentally explores the thermal resistance between bolted and clamped TO-220 packages and the heat sink due to the electrical insulator. Aluminum oxide insulators are experimentally compared to commercially available polyimide thermal interface materials (TIMs). Various TIMs are explored to reduce the thermal contact resistance at the alumina/metal interface including screen printed phase change material. Results show that thermal contact resistance (TCR) at the alumina interface is significant under both clamped and bolted TO-220 diodes but can be reduced up to 70% with graphite sheets, thermal grease or phase change material.

Nomenclature

A	apparent contact area [m^2]
D	bolt diameter [m]
D_{bv}	dielectric breakdown voltage [V]
f	friction factor
F	force [N]
T	torque [$N \cdot m$]
I	electrical current [A]
P	average contact pressure [Pa]
P_e	electrical power [W]
R	thermal resistance [K/W]
$\dot{Q}$	heat transfer rate[W]
T_d	diode leadframe temperature [K]
T_{cp}	cold plate temperature [K]
u	absolute uncertainty
V	voltage [V]
ε_0	permittivity of free space [F/m]
ε_R	relative permittivity
σ	standard deviation

1. Introduction

To meet CO2 reduction goals, the world is phasing out fossil fuels and replacing them with renewable electrical energy. According to the International Energy Agency, the auto industry will need to put 20 million electric and plug-in hybrid electric vehicles (EV/HEV) on the road by 2050 and global capacity of 1,600 GW of wind and 1,700 GW of solar photovoltaics are required by 2030 [1]–[3]. These technologies require low cost and reliable power electronics for electrical energy conversion [4]. For example, electric vehicles require battery chargers, DC-DC converters and electric motor drives.

Power diodes and transistors, integrated either in power modules or as individual discrete packages, are among the most common components in these systems [5]. The lower cost transistor outline (TO) series components, such as the TO-220 and TO-247, are widely used in lower current applications such as on-board electric vehicle battery chargers. When operating at high voltage they require electrical insulation before mounting onto touch-safe heat sinks. The electrical insulation adds additional thermal resistance to the heat transfer from device to ambient. In some cases, the electrical insulation may represent the largest thermal resistance in the heat path. Increasing thermal resistance without decreasing power results in an increase in device temperature which in turn results in an exponential increase in device failure rate [6]. Common electrical insulators include polyimide films coated with thermal interface materials (TIMs) to reduce the thermal contact resistance (TCR) developed between both imperfect contact interfaces (device/insulator and insulator/heat sink) [7], [8]. Alternatives to polyimide films include ceramics which, as seen in Table 1, have thermal conductivities orders of magnitude larger than most dielectrics [9]. However, since they have lower dielectric strengths than other dielectrics, ceramics used to isolate high voltage devices must be relatively thick. This additional thickness is beneficial in reducing electric capacitance between device and heat sink, which can mitigate common mode electromagnetic interference (EMI) noise from high frequency power device switching.

Low cost ceramic insulators, such as alumina, are not usually sold with integrated coatings or TIMs. Alumina is a hard material and thus will suffer from high TCR when in bare contact with metals. When ceramics are used to isolate discrete TO devices a reduction in bulk thermal resistance may therefore be offset by an increase in TCR.

Material	Thermal conductivity [W/m·K]	Dielectric strength [kV/mm]	Relative permittivity
Beryllium oxide	40 to 210	13	6.8
Aluminum nitride	170 to 220	10 to 15	8.7 to 16
Aluminum oxide	10 to 34	10 to 17	9.5 to 10
Polyimide film	0.1 to 1.2	120 to 300	3.5

Table 1: Typical electrical insulation properties [9], [14], [15]

In the literature, most TCR studies have focused on bare and TIM filled metal to metal contact [10]. Chung et al. studied alumina and aluminum contacts with different metallic coatings. Their results showed that aluminum and copper coatings were the most successful at reducing the TCR [11]. They did not investigate other TIMs. Many studies have been published on the thermal performance of TIMs in the literature, some of which electrically insulate adequately for high voltage applications [7], [12], [13]. However, studies on dielectric TIMs are not common and to the authors' knowledge only a few studies have been published on TIMs with alumina as a contact material. In practice, when alumina is used in industry thermal grease is applied on the surfaces to reduce the TCR. It is known that thermal grease may pump out during operation and this may result in failure if not considered [12]. In addition, the application of thermal grease or any TIM to the alumina adds an additional manufacturing step on the assembly line.

In this work, a phase change material (PCM) TIM is screen printed onto both sides of an alumina insulator. The PCM and screen printing is provided by a thermal management supplier [Universal Science, Milton Keynes, United Kingdom]. It is believed that this alumina/PCM insulator will be more easily and reliably installed into a product on the assembly line than insulators with separate TIMs. The thermal resistance of the alumina insulator with screen printed PCM is measured under a TO-220 diode bolted and clamped to an aluminum heat sink. Commercially available polyimide insulators and various other TIM and alumina combinations are also tested in the same configurations.

2. Experimental Setup

Figure 1 shows a schematic of the custom-designed test bed. Thermocouples [T type, OMEGA, ±0.5°C] are epoxied to a TO-220 dual Schottky diode [100 V, ON Semiconductor] and to a custom-built water-cooled aluminum cold plate finished with a fly cutter on a mill and then polished with 400 grit sand paper. A thermal bath [Polystat 3C15, Cole Parmer] is used to cool the cold plate. The diode package is soldered to a printed circuit board (PCB) to facilitate splitting the connected power cables. The cables are connected to a programmable DC power supply [62012p-80-60, Chroma], and two additional wires are attached to the PCB traces next to the diode leads for voltage measurement across one of the two diodes in the TO-220 package. Control and data acquisition are performed using a desktop computer and a data acquisition module [NI CDAQ-9174, National Instruments] containing cartridges for recording thermocouple [NI 9213, National Instruments] and voltage measurements [NI 9205, National Instruments].

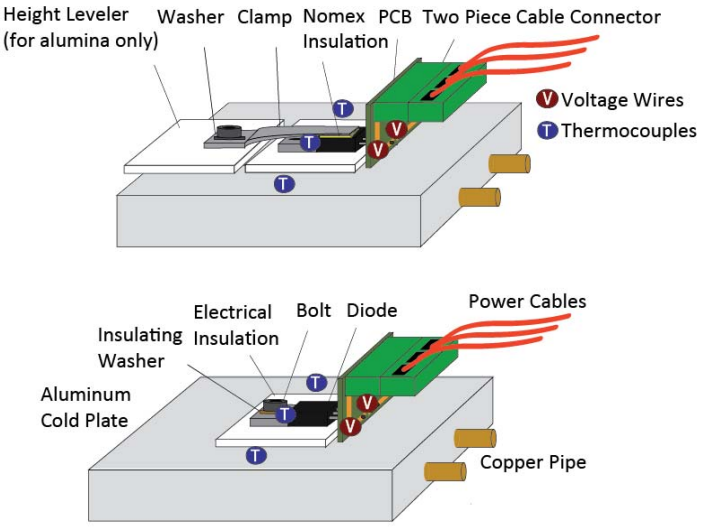

Fig. 1: Experimental Setup

Current is read from the power supply and recorded automatically by the control program written in LabVIEW. Prior to mounting, the cold plate surface is lightly rubbed with steel wool to remove any oxide layers and then both diode and cold plate are cleaned with isopropyl alcohol. The diode, washer and insulating material are mounted using an M3 bolt torqued to 0.56 N-m (5 in-lbs). For the clamped configuration, insulating paper (Nomex) is used between the bolted clip and the diode. To maintain the same clamping force, a bare alumina height leveler is placed under the clip when alumina is used to isolate the diode. After mounting, the cold plate is then insulated from the environment using glass wool and the power is turned on. Power supply voltage and current, diode voltage, diode temperature and cold plate temperature are recorded once steady-state is achieved. This is determined to be when temperature and voltage rates of change are below a certain threshold (1.25x10^-5) for a certain period of time (3 minutes). Extending the steady-state parameters had no significant effect on the results.

Cold plate and alumina surface characteristics are provided in Table 2. Roughness and flatness deviation were measured using a profilometer (skidless diamond tip, Mitutoyo Surftest SJ-400, flatness resolution of 0.3 μm over 25 mm) after all thermal resistance measurements were conducted. The relatively large out-of-flatness of the cold plate along the width of the diode is due to the manual steel wool rubbing between runs.

Sample	Root mean square roughness, R_q [µm]	Peak to peak maximum out-of-flatness deviation [µm]
Cold plate (along width of diode)	0.4	21.1 (concave)
Cold plate (along length of diode)	0.4	5.3
Alumina insulator	1.1	10.6

Table 2: Average roughness and flatness measurements of contact surfaces

Electrical power is calculated using Eq. 1 by assuming both diodes in the TO-220 have the same voltage drop and that the voltage drop in the leads, solder and traces in the PCB are negligible.

$$\dot{Q} = P_e = \Delta V \cdot I \quad (1)$$

Thermal resistance is calculated using Eq. 2 by assuming that the temperature gradient in the aluminum cold plate is negligible compared to the temperature difference between the diode and the cold plate. In addition, losses to the ambient through the insulation and through the power cables are neglected.

$$R = \frac{T_d - T_{cp-avg}}{\dot{Q}} \quad (2)$$

3. Electrical Insulation and TIM Sample

Materials used to electrically insulate the diode from the cold plate are listed in Table 3. These materials are commercially available and were selected based on recommendations from an industrial partner of the project [Delta-Q Technologies, Burnaby BC Canada]. Though the list is not exhaustive, these products were selected because of their reasonable cost and frequent use in high voltage power electronics. All dielectrics used provide at least 4,000 V of dielectric breakdown voltage. Also included in Table 3 are one dimensional thermal resistance, parallel plate capacitance and dielectric breakdown voltage. Breakdown voltage, thermal conductivity and thickness are reported by the manufacturer while relative permittivity is approximated. Capacitance and thermal resistance are calculated using Eq. 3 and 4. The alumina insulator chosen has a dielectric breakdown voltage at least four times higher than the polyimide films and yet still has the lowest expected thermal resistance and capacitance. Decreasing the alumina thickness would result in even lower thermal resistance but higher capacitance.

$$C = \frac{\varepsilon_0 \cdot \varepsilon_r \cdot A}{t} \quad (3)$$

$$R_{1D} = \frac{t}{k \cdot A} \quad (4)$$

Commercially available TIMs used to reduce the TCR introduced by the alumina are listed in Table 4. Unique samples, developed to reduce assembly time, are shown in Fig. 2. The samples were created by screen printing phase change material onto both sides of the alumina insulators.

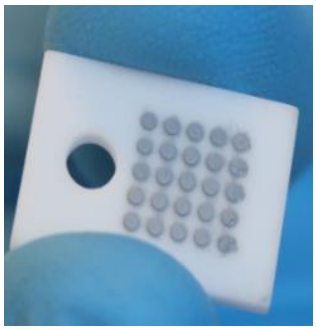

Fig. 2: Screen printed PCM onto alumina insulator [Universal Science, Milton Keynes, UK]

Alumina TIMs	Thermal conductivity [W/(m·K)]	Thickness [mm]
Synthetic graphite 400	400 (in-plane) 28 (through-plane)	0.2
Synthetic graphite 700	700 in-plane	0.1
Silicon-based thermal grease	2.3	-
Cured gap filler	3.6	-
Screen printed PCM on alumina	3.5	-

Table 4: Reported properties of non-electrically insulating TIMs for alumina

Electrical insulator	Thermal conductivity [W/(m·K)]	Dielectric breakdown voltage [V]	Relative permittivity	Thickness [mm]	1D Thermal resistance [K/W] (1 cm x 1 cm)	Parallel plate capacitance [pF] (1 cm x 1 cm)
Adhesive coated polyimide tape	0.40	6,000	3.5	0.203	5.00	15.5
PCM coated polyimide film	0.46	4,200	3.5	0.05	1.08	61.9
Alumina	15	26,533	10	1.57	1.04	5.64

Table 3: Properties of electrically insulating samples

4. Experimental Results

Thermal resistance results for a TO-220 diode bolted and clamped with electrical insulation are provided in Fig. 3. The experimental uncertainty, which is plotted as error bars, includes both calculated uncertainty and the standard deviation of the measurements. The standard deviation of the alumina without any TIM is much higher than for the other samples. This may be due to mounting misalignment, mounting pressure variation and changes in the surface of the diode and the cold plate with individual runs. When TIMs are used high standard deviation is not observed as the conforming material reduces the result's dependency on pressure, roughness and non-conformity of the contact. Uncertainty analysis equations are shown in Eq. 5 through 8.

$$\frac{u_{\dot{Q}}}{\dot{Q}} = \sqrt{\left(\frac{u_{\Delta V}}{\Delta V}\right)^2 + \left(\frac{u_I}{I}\right)^2} \quad (5)$$

$$u_{\Delta T} = \sqrt{(u_T)^2 + (u_T)^2} \quad (6)$$

$$\frac{u_R}{R} = \sqrt{\left(\frac{u_{\Delta T}}{\Delta T}\right)^2 + \left(\frac{u_{\dot{Q}}}{\dot{Q}}\right)^2} \quad (7)$$

$$u_{R\cdot\sigma} = \sqrt{(u_R)^2 + (\sigma)^2} \quad (8)$$

The thermal resistances range from 0.65 K/W for a bare un-insulated diode up to 4.1 K/W when the diode is insulated with adhesive coated polyimide tape. Alumina, without any TIM, is the second worst insulator tested. The alumina insulators have a lower thermal resistance than the polyimide films tested however the high TCR at both the diode and cold plate interface results in a higher total thermal resistance. The polyimide films are both coated with a material that reduces this TCR. When thermal grease, gap filler, graphite or PCM is used on both sides of the alumina the reduction in thermal resistance is as high as 70% which confirms that TCR is a major bottleneck to heat flow on alumina interfaces. Performance differences between the TIMs used are not discernible on this testbed as the error bars are overlapping. Relatively thick layers of grease and gap filler were used on the alumina surfaces. This may have been required due to the large out-of-flatness of the cold plate surface. The average pressure distribution under the diode is shown for both diode configurations in Table 5. The average pressure under the bolted configuration is an approximation calculated using Eq. 9 and 10 with a friction factor of 0.2.

$$F = \frac{T}{f \cdot D} \quad (9)$$

$$P = \frac{F}{A} \quad (10)$$

Only Eq. 10 is necessary for the clamped configuration where it is assumed the applied force is equal to the rating of the clip (50N).

Configuration	Average pressure under diode [kPa]	Average pressure under alumina [kPa]
Bolted 0.56 Nm	6,517	3,260
Clamped 50 N clip	333	167

Table 5: Average pressure distribution at TO-220/alumina and alumina/cold plate interfaces

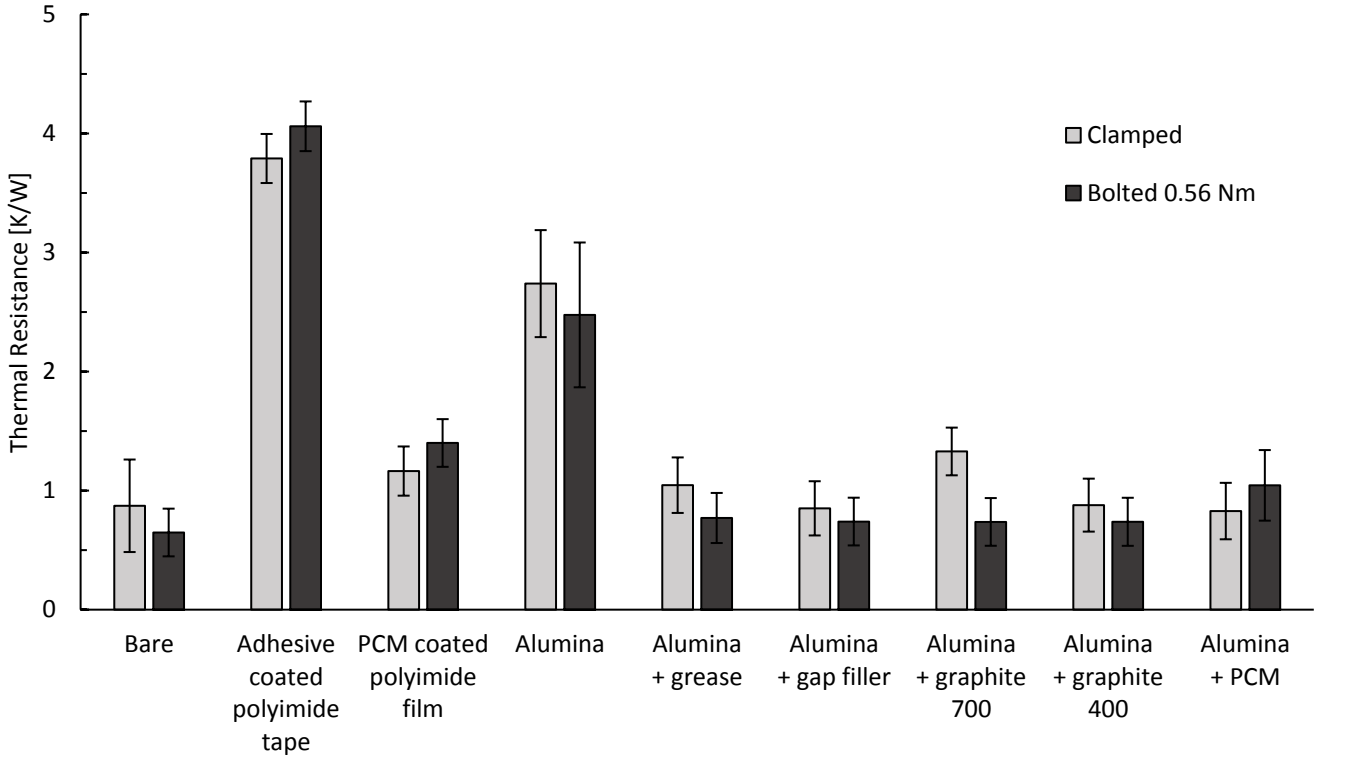

Fig. 3: Thermal Resistance of TO-220 power diodes clamped and bolted with electrically insulating thermal interface materials.

Despite the different contact pressures, the experimental results show that there is no discernible thermal difference between clamped and bolted TO-220s when using electrical insulation as the differences fall within the error bars. This may be because under the bolted configuration, the average non-uniform contact pressure is higher than the clamped configuration but it is located further from the die location in the package. In both setups, heat may bypass the insulating TIM and travel through the bolt or the clip assembly. The differences in thermal resistance of these paths may also influence the result. Differences in thermal resistance due to temperature were not discernible on this testbed.

5. Conclusion

Results for the thermal resistance of a bolted and clamped TO-220 with screen printed PCM on alumina as electrical insulation are presented along with commercially-available insulator and TIM combinations. No discernible differences are observed between the clamped and bolted configurations despite the different contact pressures in both configurations. The alumina with TIM combination was competitive with respect to the commercially available polyimide film products despite offering higher breakdown voltage and lower capacitance. Its thermal resistance approaches that of the bare TO-220 without a TIM. To reduce experimental error, standardized tests are recommended for further quantifying the differences between TIMs and electrical insulators used for power packages. Cyclical pump-out tests, PCM array optimization and more detailed surface characterization are also recommended in the future.

Acknowledgements

The authors would like to thank James Stratford of Universal Science for screen printing the PCM onto the alumina and Dr. Wendell Huttema for his guidance and help with the experimental setup.

References

[1] International Energy Agency IEA, "Technology Roadmap: Electric and plug-in hybrid electric vehicles," Paris, 2011.

[2] International Energy Agency IEA, "Technology Roadmap: Wind energy," Paris, 2013.

[3] International Energy Agency IEA, "Technology Roadmap: Solar Photovoltaic Energy," Paris, 2014.

[4] R. K. Dey and A. Sardar, "Trends in Power Electronics Packaging Technologies For XEVs," *Auto Tech Review*, vol. 3, no. 8, pp. 18–23, Aug. 2014.

[5] Y. Xiong et al., "Prognostic and Warning System for Power-Electronic Modules in Electric , Hybrid Electric , and Fuel-Cell Vehicles," *IEEE Transactions on Industrial Electronics,* vol. 55, no. 6, pp. 2268–2276, 2008.

[6] Y. A. Cengel, *Heat Transfer A Practical Approach*, 2nd ed. New York: McGraw-Hill, pp.787, 2004.

[7] D. Gautam, D. Wager, M. Edington and F. Musavi, "Performance comparison of thermal interface materials for power electronics applications," *2014 IEEE Applied Power Electronics Conference and Exposition - APEC 2014*, Fort Worth, TX, pp. 3507–3511, 2014.

[8] M. Bahrami, M. M. Yovanovich, and E. E. Marotta, "Thermal joint resistance of polymer-metal rough interfaces," ASME. *J. Electron. Packag.*, vol. 128, no. 1, pp. 23–29, 2006.

[9] X. C. Tong, *Advanced Materials for Thermal Management of Electronic Packaging*. Springer-Verlag New York, 2014.

[10] M. M. Yovanovich, "Four decades of research on thermal contact, gap, and joint resistance in microelectronics," *IEEE Transactions on Components and Packaging Technologies*, vol. 28, no. 2. pp. 182–206, 2005.

[11] K. C. Chung, H. K. Benson, and J. W. Sheffield, "Thermal contact conductance of ceramic substrate junctions," ASME. *J. Heat Transfer*, vol. 117, no. 2, pp. 508–510, 1995.

[12] J. Hansson, C. Zanden, L. Ye, and J. Liu, "Review of current progress of thermal interface materials for electronics thermal management applications," *2016 IEEE 16th International Conference on Nanotechnology (IEEE-NANO),* Sendai, pp. 371–374, 2016.

[13] K. C. Otiaba, N. N. Ekere, R. S. Bhatti, S. Mallik, M. O. Alam, and E. H. Amalu, "Thermal interface materials for automotive electronic control unit: Trends, technology and R&D challenges," *Microelectronics Reliability*, vol. 51, no. 12. pp. 2031–2043, 2011.

[14] T.-L. Li and S. L.-C. Hsu, "Enhanced thermal conductivity of polyimide films via a hybrid of micro- and nano-sized boron nitride," *J. Phys. Chem. B*, vol. 114, no. 20, pp. 6825–6829, 2010.

[15] R. C. Buchanan, "Ceramic Insulators," in *Ceramic Materials for Electronics*, Third, Rev., R. C. Buchanan, Ed. New York: Marcel Dekker, 2004, pp. 1–85.